A STATISTICAL AND PARAMETRIC ANALYSIS OF THE EFFECTIVENESS OF DIFFERENTIAL DRAG FOR COLLISION AVOIDANCE MANOEUVRES

Daniele Bella[(1)], Andrew Ratcliffe[(2)], Vitali Braun[(3)], Stijn Lemmens[(4)]

[(1)] Previously Seconded to UK Space Agency from European Space agency; now IMS Space Consultancy GmbH, Robert-Bosch-Straße 7, 64293 Darmstadt, Germany, Email: d.bella@ims-space.com
[(2)] UK Space Agency, Quad Two Building (1st Floor), Rutherford Avenue, Didcot, Oxfordshire, OX11 0DF, United Kingdom, Email: andrew.ratcliffe@ukspaceagency.gov.uk
[(3)] IMS Space Consultancy GmbH, Robert-Bosch-Straße 7, 64293 Darmstadt, Germany, Email: v.braun@ims-space.com
[(4)] European Space Agency, ESA-ESTEC, 2200 AG Noordwijk, Netherlands, Email: stijn.lemmens@esa.int

ABSTRACT

The execution of collision avoidance manoeuvres (CAMs) in low Earth orbit (LEO) is increasingly important, but the implementation of propulsion systems can have significant system costs. Differential drag presents itself as an alternative, allowing for long-term modifications of the trajectory through changes in the ballistic coefficient. The European Space Agency's Assessment of Risk Event Statistics (ARES) tool has recently implemented equations to statistically quantify the effectiveness of this manoeuvring method. This paper presents an initial parametric exploration of this capability. The results suggest that differential drag can be very effective for smaller satellites up to around 550km altitude, but major differences to the results found in literature suggests that further analysis is required.

1 INTRODUCTION

With the increase in the number of objects in low Earth orbit (LEO), effective implementation of collision avoidance manoeuvres (CAMs) is becoming more and more critical. For detectable objects, CAMs are the only method available to reduce the risk of collisions, as they are typically too large to shield against. [1]

Manoeuvres of this kind traditionally require a propulsion system in order to impart a change in velocity (ΔV) to the spacecraft. This trajectory change can then be optimised in order to reduce the probability of collision P_c.

If the thrust of the system is high enough, as is typically the case for chemical propulsion, the propulsion system can be approximated to be "impulsive" i.e. the force it generates can be approximated as an instant change in velocity to the spacecraft.

More recently, low-thrust propulsion systems have risen in popularity due to their increased fuel efficiency, which instead need between hours and days to perform manoeuvres. For CAMs in particular, this imposes a minimum manoeuvre duration Δt_{man} and thus decision lead time Δt_{dec}, below which a sufficient decrease in P_c cannot be guaranteed.

However, even low-thrust propulsion systems can have significant system costs for small satellites, and their mass can be a significant percentage of that available for the spacecraft platform. Often, the inclusion of these systems is driven by the need to perform CAMs [2]. This drives the need to find alternative methods to reduce the probability of collision and risk to the environment, without the need for these systems [3].

An alternative that is showing promise is differential drag. This is the modification of the predicted trajectory through the alteration of the drag force affecting the spacecraft. This can be for instance achieved through a change in spacecraft attitude, and the subsequent change in the effective drag cross-sectional area A. A great advantage of this method is that it can in principle be accomplished without a propulsion system, allowing for manoeuvres without any consumables.

Differential drag has benefitted from several studies looking at its use during commissioning, in order to achieve a required phase difference between spacecraft in a constellation. This has also been applied in practice; examples include the *Cyclone Global Navigation Satellite System* (CYGNSS) [4], and Planet Labs' *Dove* spacecraft [5].

However, the drag force scales with atmospheric density, and thus tends to be very small for spacecraft in LEO. This also makes the available trajectory control authority subject to very large variations, both with the altitude and with the solar activity [6]. These factors make it much harder to apply differential drag to the strict timeframe of at most a few days needed for a CAM [7], and the conditions in which this is effective remain a topic of research.

Much of the work has been driven by Planet Labs, who to the knowledge of the authors represent the only operational use of differential drag for collision

Proc. 9th European Conference on Space Debris, Bonn, Germany, 1–4 April 2025, published by the ESA Space Debris Office
Editors: S. Lemmens, T. Flohrer & F. Schmitz, (http://conference.sdo.esoc.esa.int, April 2025)

avoidance in a fleet [8]. Few other attempts to demonstrate or test its effectiveness in orbit were found in the literature, and neither led to operational usage [9] [10].

However, simplified analytical equations were created in order to assess the possible change in trajectory and therefore viability of a differential drag CAM. These equations allow for the complex problem of orbit propagation for CAM design to be approximated analytically, removing the need for a computationally costly numerical propagation [10]. Through work by other authors, the scope of these equations was expanded, allowing for the reduction in P_c to be directly calculated [6].

These have however only been run for single events, looking at the effectiveness for very specific test cases. Another approach is to take a statistical viewpoint, and to assess how effective differential drag would be on average if applied to a representative range of events. If this analysis is run parametrically, it could also identify the regimes, operational profiles and satellite geometries for which differential drag can be seen as a viable option, providing inputs to both system designers and regulatory bodies.

This type of analysis has been performed only in [11], where CDMs were processed using NASA's Maneuver Trade Space (MTS) tool to analyse how often it can be expected for a change in (inverse) ballistic coefficient β to result in a sufficient decrease in P_c. Results were also drawn on the altitudes where differential drag can be considered as effective, and the relative change in β that would be needed. It also explores the variables that contribute to the effectiveness of differential drag, and gives recommendations on when it should be considered operationally [11]

ESA has a dedicated tool for performing statistical analyses for collision avoidance: *Assessment of Risk Event Statistics* (ARES), one of the modules of ESA's *Debris Risk Assessment and Mitigation Analys*is (DRAMA). For a given operational profile, satellite, and orbit, ARES can for instance calculate the expected annual number of CAMs M_A, the associated ΔV requirements, the annual collision risk reduction due to performing CAMs Q, and many other useful metrics for spacecraft designers and analysts. [12]

In order to do this, it uses a simplified detectability equation to assess the proportion of the space debris population that the spacecraft would in principle be able to perform a CAM against. From there, it leverages ESA's Conjunction Data Message (CDM) database and the MASTER population to derive statistics for the analysed missions, by applying averaged conjunction geometries and conditions. [12]

As part of the new developments introduced in DRAMA version 4.0, ARES will implement the capability to perform calculations for differential drag CAMs. This will allow for the effectiveness of differential drag to be assessed statistically by mission designers. [13]

Whilst the analysis in [11] is a very promising first look at the statistical and parametric analysis of differential drag collision avoidance manoeuvres, the recent implementation of differential drag into ARES provides an opportunity to cross-check the results obtained, as well as derive additional results for other operational profiles, satellites and orbits. This will be explored in this paper, exploring the alternative approach and the relative differences.

1.1 Notes on Operational Implementation of Differential Drag

Whilst this paper will focus on theoretical capabilities based on available models, this brief section on operational factors and limitations nevertheless included so as to give a more complete picture of the system-level issues one might have to face if implementing differential drag.

Firstly, it is important to note that the drag coefficient C_D used operationally will be typically different to that which is assumed during the design. In contrast to the design value, found through analysis or simply assumed, the operational value will have been solved for as part of the orbit determination process, and can be very different. For planning effective differential drag CAMs, it would thus be crucial to use the operational C_D value to accurately predict a new trajectory. Alas, this operational C_D takes time to find and refine, potentially leading to delays before the first effective differential drag manoeuvre can be performed, complicating compliance with space debris mitigation (SDM) requirements [2].

Additionally, unless informed otherwise, the orbit determination process used by Space Situational Awareness (SSA) providers typically assume a constant inverse ballistic coefficient β. Thus, a spacecraft who frequently and systematically varies β could decrease the quality of the orbit predictions created by this SSA provider, complicating coordination between operators, and thus potentially reducing any environmental benefits of being able to perform CAMs. This further reinforces the need for predictive ephemerides to be shared by operators, especially if differential drag manoeuvres are foreseen.

Finally, from a practical perspective, the simplest way to achieve a change in the ballistic coefficient is to modify the attitude of the spacecraft. However, on top of the potential effect on payload availability, a typical spacecraft platform might not be able to keep an off-nominal attitude for hours or days at a time. This was shown in [9] and [14] who had their spacecraft enter safe mode multiple times when trying to perform an in-orbit demonstration of a differential drag manoeuvre. This can of course be mitigated during the design phase but nevertheless complicates applying differential drag as a contingency or to an already flying mission.

2 METHODOLOGY

In this section, an overview of the methodology for this analysis will be presented.

The debris population used for all these analyses is the validated 2016 MASTER population, as at the start of the project it was the most recent one available.

2.1 Differential Drag Manoeuvre Modelling

Differential drag is implemented into DRAMA through the equations derived in [10]. These leverage several key assumptions:

- The change in position at TCA is exclusively in the along-track direction, and not along the cross-track and radial directions.
- The orbit of the target is circular.
- The change in semi-major axis due to the manoeuvre is small.

After some derivation presented in [10], these assumptions lead to Eq. 1.

$$\ddot{\phi} = -\frac{3\rho_0\mu_E}{a_0^2}\Delta\beta_{CAM} \tag{1}$$

Where:

- $\ddot{\phi}$ is the second derivative with respect to time of the mean anomaly of the target
- ρ_0 is the averaged atmospheric density along the orbit of the spacecraft
- μ_E is the gravitational parameter of the Earth
- a_0 is the semi-major axis of the target
- $\Delta\beta_{CAM} = \beta_{man} - \beta_{nom}$ is the change in inverse ballistic coefficients between nominal and manoeuvre modes.

It is important to note that, for this analysis, the inverse ballistic coefficient is defined as in Eq. 2.

$$\beta = \frac{C_D A}{m} \tag{2}$$

Where m is the mass of the spacecraft, C_D is the drag coefficient, and A is the cross-sectional area of the spacecraft in the relevant direction.

Eq. 1 effectively turns the problem of evaluating the effectiveness of a CAM into a differential equation, allowing for the final change in mean anomaly, and thus the post-CAM miss distance to be evaluated by simple integration with respect to time.

Within ARES, if differential drag evaluation is selected by the user, Eq. 1 is used to determine how long such a CAM would take, and compares that result to the inputted decision lead time Δt_{dec}. If it is found that a differential drag CAM would be possible within this time constraint, the current implementation marks the ΔV from that manoeuvre as deductible This allows the user to statistically assess how much ΔV could be saved by implementing differential drag on top of a standard manoeuvring methodology.

For the purposes of this study, this implementation was expanded to be able to assess the capabilities of a spacecraft solely using differential drag i.e. if it was found using the aforementioned methodology that a differential drag CAM would not be possible, the manoeuvre information was logged. Once the analysis was performed for all CAMs and combined statistically, the end result is the number of manoeuvres *missed* $\bar{M}_{DD}$, and the amount of risk reduction that *cannot* be achieved when solely using differential drag $\bar{Q}_{DD}$.

These values are however hard to interpret, due to the double negation involved. Thus, in order to be able to more effectively compare impulsive and differential drag manoeuvres, the manoeuvre and risk reduction figures of merit η_M and η_Q were constructed, using as reference the impulsive manoeuvre rate M_A and risk reduction Q respectively. These can be found expressed in Eqs. 3 and 4.

$$\eta_M = 1 - \frac{\bar{M}_{DD}}{M_A} \tag{3}$$

$$\eta_Q = 1 - \frac{\bar{Q}_{DD}}{Q} \tag{4}$$

η_M and η_Q can be thought of as efficiencies, with a value between 0 and 1; $\eta = 1$ implies that differential drag would be just as effective as impulsive manoeuvres in the same scenario, and $\eta = 0$ corresponds to no effectiveness at all. In order to increase their legibility, they will be presented as percentages for the remainder of this paper.

2.2 Test Cases

Due to the number of input parameters needed, it was decided to analyse specific test cases, rather than perform a full parametric sweep of every variable.

Thus, three test cases were chosen. Due to their accessibility, values based on previous demonstrations or tests of differential drag were preferentially chosen.

The first case was selected due to the general suitability of the differential drag concept to CubeSat satellites. Their low mass and tight volume constraints mean that propulsion systems can be particularly difficult to implement, and potentially lower payload availability requirements mean that longer manoeuvres would not be as much of a concern.

The particular CubeSat that was chosen is based on ESA's OPS-SAT satellite, a 3U CubeSat featuring two deployable solar panels on either side of the long main body, which compared to the small cross-section of its slender body, provide an impressive maximum area of 0.115 m^2. [15]

The next case is slightly larger, created by merging the properties of several similar satellites: TET-1 [14] and the Flying Laptop [6]. This allowed for the "small satellite" case to be created. This test case also has a dual solar panel arrangement, but due to the less elongated body, the change in inverse ballistic coefficient is not as dramatic as for the CubeSat case.

Finally, a much larger case was also chosen, based on NASA's EO-1 spacecraft [9]. In contrast to the others, this spacecraft features a cylindrical body with a long, trailing solar panel.

In the CubeSat and Large satellite cases, a C_D of 2.2 was assumed; whilst this is not generally a valid assumption for fixed attitudes, due to lack of other data and the generic analysis, it was considered sufficient as a first approximation.

In terms of geometry, whilst the satellite structure defines the maximum and minimum inverse ballistic coefficient β_{max} and β_{min}, the "nominal" inverse ballistic coefficient β_{nom} needs to be defined. Its relevance comes from the fact that differential drag relies on a deviation from the *nominal* trajectory, and that for the same reduction in P_c, CAMs can require different amounts of. Thus, if a spacecraft is always in a configuration where $\beta = \beta_{min}$ or $\beta = \beta_{max}$, that will preclude manoeuvring in a certain direction, potentially limiting the effectiveness of CAMs it can produce.

The true β_{nom} will of course depend on the design, mission and operational profile of each individual satellite. In [11], as it was assumed that the most logical way for a mission to operate was to make $\beta_{nom} = \beta_{min}$, and thus making $\beta_{man} = \beta_{max}$. As this case is quite constraining, it was decided to instead assume that that β_{nom} simply lies at the midpoint of β_{max} and β_{min}, allowing for the possible change in inverse ballistic coefficient for a CAM in either direction $\Delta\beta_{CAM}$ to be calculated as in Eq. 5.

$$\Delta\beta_{CAM} = \frac{\beta_{max} - \beta_{min}}{2} \tag{5}$$

To summarise, an overview of the properties of the three final test cases can be found in Tab. 1, and an illustration of what different attitudes represent can be found graphically in Fig. 1.

Table 1: Overview of test case properties

	CubeSat	**Small Satellite**	**Large Satellite**
Based on	OPS-SAT (3U) [15]	Flying Laptop [6], TET-1 [14]	EO-1[9]
m [kg]	5	120 [14]	573
HBR [m]	0.5	0.75 [14]	2.5
A_{min} [m^2]	1.51E-02	-	2.86
A_{max} [m^2]	1.55E-01	-	8.04
β_{min} [$m^2\,kg^{-1}$]	6.64E-03	1.21E-02 [6]	1.10E-02
β_{max} [$m^2\,kg^{-1}$]	6.82E-02	3.26E-02 [6]	3.09E-02
$\Delta\beta_{CAM}$ [$m^2\,kg^{-1}$]	3.08E-02	1.03E-02	9.94E-03

2.2.1 Assumed Orbital Parameters

In order to be able to gauge the effectiveness of differential drag, a parametric sweep of different altitudes h and thus semi-major axes $a = R_E + h$ is performed, where $R_E \approx 6378.1$ km is the average radius of the Earth. Within this paper, the parameter range 300 km $\leq h \leq$ 800 km is used, with a step of 25 km.

In line with the assumptions of Eq. 1, and also keep the problem tractable, near-circular orbits are assumed for this analysis i.e. the eccentricity $e \approx 0$.

Two values of the inclination i are chosen for these initial simulations; the first corresponds to a fixed $i = 53°$, and the second corresponds to the inclination needed for a Sun-Synchronous Orbit at each altitude.

The right-ascension of the ascending node and the mean anomaly are not taken into account by ARES and are averaged; thus, arbitrary values were chosen.

2.2.2 Assumed Operational CAM Procedure

Typically, spacecraft will have a defined decision period prior to TCA Δt_{dec}, and a defined Acceptable Collision Probability Level (ACPL). If the $P_c > ACPL$ and $\Delta t_{TCA} < \Delta t_{dec}$, then a CAM is performed, aiming to reduce the P_c below the target value.

One of the intricacies of CAM design is that, even for the same spacecraft and event, there are many different ways one can implement a CAM. As an example of a trade-off, a later manoeuvre benefits from refined data and smaller propagated covariances but can require more ΔV. This becomes even more complex for low-thrust manoeuvres, as the possibility of splitting the manoeuvre into distinct bursts becomes possible. [6][11].

In practice, the selected approach would be decided based on the specific spacecraft's operational requirements, and on the mission plan.

However, for this study, since the aim is to quantify the limits of what *could* in principle be achieved, it was decided to assume that a CAM is applied immediately at decision time, and that the manoeuvre lasts until TCA. In practice, this means that the manoeuvre inverse ballistic coefficient has a constant value $\beta_{man} = \beta_{nom} \pm \Delta\beta_{CAM}$, with the direction in which $\Delta\beta_{CAM}$ is applied decided based on the event geometry. This approach is the one that allows for the smallest Δt_{dec} possible, at the expense of potentially having a longer Δt_{man}. By extension, it follows that $\Delta t_{dec} = \Delta t_{man}$.

In terms of the values of the operational parameters, within this study Δt_{dec} is explored parametrically with a discretisation step of:

- 1 hour, for 2 hours $\leq \Delta t_{dec} <$ 12 hours
- 6 hours, for 12 hours $\leq \Delta t_{dec} \leq$ 5 days

This leads to a total of 29 simulated values of Δt_{dec}.

In permutation with this, two distinct values of the ACPL are explored as part of this study: 1E-4, and 4E-5.

Finally, the target P_c is defined as a reduction by two orders of magnitude, in line with ESA requirements [2].

2.3 Atmospheric Model and Solar Activity

Whilst the DRAMA 4.1 release implements differential drag within ARES, the atmospheric model that it implements is exponential. Due to the changes in density, solar activity was identified in [6] to have a very large influence on the amount of separation that a manoeuvre can cause, and thus it was set out to investigate it further as part of this study.

However, the input structure of ARES precludes the direct application of a complex atmospheric model. Thus, for the purposes of this analysis, a surrogate model was constructed as a compromise, allowing for the variation in solar activity to be accounted for without introducing undue complexity or significantly increasing the computational time.

The approach for constructing this atmosphere model was to first evaluate the atmospheric density at different altitudes over 10000 points, distributed on the earth using the principle of a Fibonacci sphere, in order to first create a location-averaged model. In principle, any atmospheric model could have been used to evaluate the density at the evaluation points; for this paper the NRLMSIS-2.1 model, described in [16], was chosen.

This location averaging was repeated at 8 different times of the year, in order to average the effect of the time of year.

In order to simplify the analysis, only the effect of the solar F10.7 flux was taken into account; the Ap index was assumed to be equal to a constant value of 15. All the above was thus repeated for F10.7 indices equal to 75, 100, 125, 150, 175, 200, 225, and 250.

Figure 1. Example of correspondence between inverse ballistic coefficient values, and spacecraft attitude modes

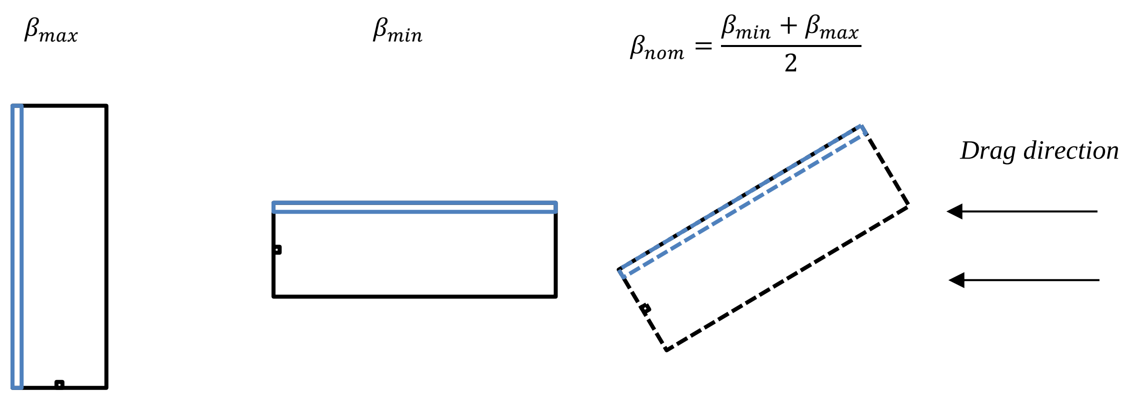

The final surrogate atmosphere model thus has inputs of only the F10.7 solar index and the altitude. The ARES simulations were run with each permutation of these, providing a snapshot of the effectiveness of differential drag based on different values of solar flux.

The final step was to collect statistics on F10.7 indices throughout different solar cycles, such as to be able to aggregate these results, and provide an "averaged" overall effectiveness; this is similar in concept to the approach dictated by [2] for evaluating the disposal lifetime, whereby the lifetime must be evaluated throughout an entire solar cycle. To perform this, statistics were drawn using the SOLMAG tool [17] on the last 5 complete solar cycles, leading to the histogram shown in Figure 2. The counts of these histograms were then used as weights for the averaging, leading to the final results shown in Section 3.

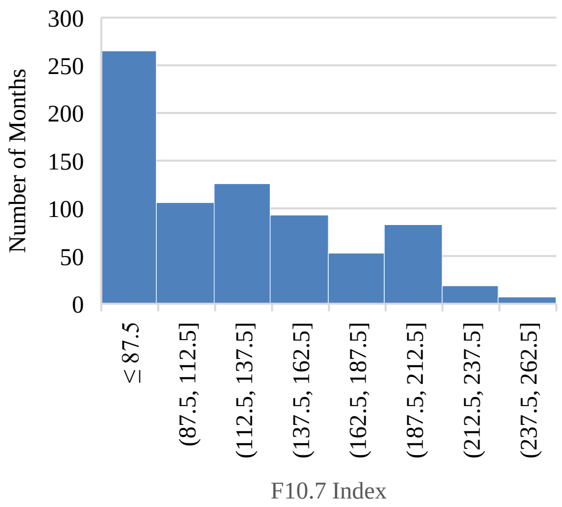

Figure 2. Statistics of F10.7 Index, drawn from solar cycles 19-24.

3 RESULTS AND DISCUSSION

Based on the methods outlined above, the simulations were run in a Linux environment. A large advantage of the ARES software is that each individual run can in principle be performed in parallel, allowing for scaling based on the available computing power.

Taking into account each permutation of the input parameters, each of the three test cases involved 19488 individual runs of ARES. In practice, for the evaluation of the effectiveness of a specific mission, the number of permutations could of course be significantly reduced. In terms of computational time, using 7 cores of an Intel(R) Xeon(R) Platinum 8462Y+ CPU, the analysis took around 15 hours to complete, and on average used around 5GB of RAM.

3.1 CubeSat

The results of the simulations for the 3U CubeSat case can be found in Figs. 4 and 5, for an inclination in SSO and an ACPL of 1E-4.

The first immediately clear trend is the decrease in effectiveness that is seen with an increase in altitude h, and with a reduction in Δt_{cam}. This is expected; an increase in h leads to a rapid decrease in atmospheric density, reducing the manoeuvre effectiveness as seen in Eq. 1. Similarly, a reduction in Δt_{cam} reduces the amount of time during which the acceleration can take effect, once again reducing the effectiveness of the CAM manoeuvre.

An important question, also raised by [11], is what constitutes an "acceptable" value of η_M and η_Q. Indeed, no SDM requirements currently impose a restriction on the reliability of CAMs [2], which would be the most straightforward way to decide on a threshold. However, even with such a reliability value set, the reliability of the spacecraft system and ground segments would need to be taken into account, complicating its application to this case. In [11], 50% effectiveness was used as a threshold for the sake of the analysis they presented; in this paper, a higher value of 95% will be used, however this is an arbitrary choice, and further work will be needed in this domain.

With this in mind, generally, for $\Delta t_{dec} > 12$ hours and $h < 500$ km, the results suggest that differential drag could have a very similar effectiveness to chemical propulsion. Above this altitude or with a shorter manoeuvre time, the effectiveness seems to quickly decrease but still remains around 85% effectiveness at $h = 600$ km and with a $\Delta t_{CAM} = 12$ hours. For longer manoeuvres, in the order of days, the results suggest that differential drag could be used even above the 800km limit of effectiveness.

Comparing Figs. 4 and 5, it can be seen that, in general, $\eta_M \leq \eta_Q$ i.e. the risk reduction effectiveness decreases slower than the manoeuvre effectiveness. This can be explained intuitively by considering that an increased covariance size can lead to a reduction in the probability of collision, in a phenomenon known as probability dilution. This increase in covariance size also means that in order to reduce the probability of collision by a certain amount, more separation has to be created. Combined, these two phenomena explain why the "easiest" manoeuvres to perform are the ones that lead to the largest decrease in the overall collision risk, explaining the trends seen in the two plots.

3.2 Small Satellite

The results of the simulations for the small satellite can be found in Figs. 6 and 7, also for an inclination in SSO and an ACPL of 1E-4.

In general, comparing these results to Figs. 4 and 5, the same general trends can be seen, though there is a general shift towards a lower effectiveness. Indeed for $\Delta t_{CAM} =$ 12 hours, the small satellite case only seems to have near-perfect effectiveness up to $h \approx 400$ km rather than 500 km. This can be explained by the lower possible change in inverse ballistic coefficient, shown in Tab. 1.

However, an interesting new behaviour can be seen at $h = 500$ km altitude. In contrast to the monotonically decreasing effectiveness that one might expect with altitude, the effectiveness drops very sharply, before recovering at higher altitudes.

From preliminary investigation, it is believed that this is caused by the shift between altitude bins within the ARES CDM database, which also occurs at 550km [12]. Further pointing to this hypothesis is a less pronounced drop of effectiveness at 350km, another boundary of the ARES binning. This would modify the values of the covariances and the encounter geometry, affecting the size of the required CAMs and thus how effectively differential drag can perform. Once again looking back at Figs. 4 and 5, this drop in effectiveness can also be noticed, though it does not have nearly as much of an effect.

Further work should investigate the ARES CDM database to ascertain the sources of these changes, as well as run a sensitivity analysis to confirm that these large variations are not due to small variations in the input parameters.

Otherwise, the same trends can be seen in terms of the relationship between risk reduction and manoeuvre effectiveness, further suggesting that the phenomenon is not linked to size or β.

3.3 Large Satellite

Finally, for the large satellite, case, for the same inclination of Sun-Synchronous Orbit and ACPL of 1e-4, the results can be found in Figs. 8 and 9.

As seen in Tab. 1, there is not much difference in the value of $\Delta\beta_{CAM}$ between the small and large satellite case; thus, one would not expect much difference when comparing Figs. 8 and 9 to Figs. 6 and 7, and this is indeed the case for $h < 500$ km.

However, there is a significant difference between the two cases above this altitude, with the large satellite case showing significantly less effectiveness. Comparing Figs. 8 and 9, there is also a more marked discrepancy between η_M and η_Q. Since the only significant difference in the inputs is the HBR, this is the suspected the source of these changes.

Similarly to the 550km drop, a more detailed analysis of ARES CDM bins would be needed to confirm this hypothesis. It is possible that a larger target HBR leads to the combined target and chaser HBR to be dominated by the target, especially for small (and poorly tracked) chasers. Thus, for an increase in HBR, these poor covariance events will have a comparatively higher increase in collision probability than those with smaller covariance. This would exacerbate the phenomenon described in Section 3.1, leading to the more marked difference between η_M and η_Q. As for why this would only occur for $h > 550$ km, this could be due to more objects being present there. In any case, further analysis would be needed to ascertain this.

3.4 Effect of other parameters

As seen in Section 2.2, other parameter combinations were run than the ones already presented in this section, allowing for their effect to be preliminarily assessed.

However, in all cases, the general trends seen in these plots were consistent with what was already reported. These will therefore not be rediscussed, and not all generated plots will be shown in this paper.

3.4.1 Effect of Solar Cycle

Since the analysis was run for several values of the F10.7 index, it is possible to individually look at the results of each, before the averaging based on historical trends. An example of these individual results is shown in Fig. 3.

As one might expect, the solar flux has a very large effect on the effectiveness of differential drag, quasi-linearly shifting maximum effective altitude by 200 km between low and high conditions, though it should be noted that the high conditions are comparatively much rarer. This further justifies the need to model the solar cycle when assessing the effectiveness of differential drag, both during the design phase and for operational usage.

With these results in mind, it is however important to note that ARES does not take into account the variation in spacecraft covariances due to the change in solar cycle. The effects of this would however be important to explore further, as they could have significant effects on the results.

3.4.2 Effect of Inclination

Fig. 10 contains the results of running the Small Satellite test case identically to Fig. 6, with the exception of the inclination i, which is instead set to a fixed value of 53°. Comparing the two, the results are very similar, with the simulation at $i = 53°$ showing slightly lower performance overall. The results largely remain within a couple hours of Δt_{CAM} from each other, with the exception of the region $h > 650$ km, where the difference rises to around half a day of manoeuvring.

Unfortunately, due to the location averaging described in Section 2.3, the approach used for the atmospheric model does not take into account the effect of the diurnal bulge

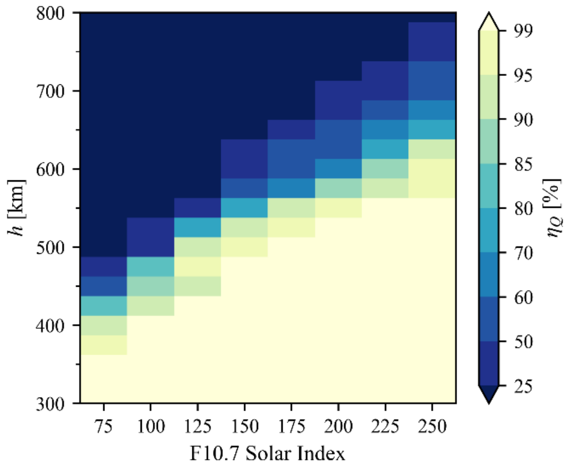

Figure 3. Percentage of CAMs that are possible when solely using differential drag for various values of the solar flux, for the small satellite test case, $i = SSO$, ACPL=1E-4, $\Delta t_{CAM} = 8$ hours

on the effectiveness of the manoeuvres, which would influence the results based on the inclination of the target's orbit. This could be resolved through directly averaging the atmospheric density along the target orbit, in line with what is recommended in [10].

3.4.3 Effect of ACPL

Fig. 11 shows the effect of running the same parameters as Fig. 6, but with an ACPL of 4E-5 rather than 1E-4.

This reduction in the ACPL also shows a slight decrease in the effectiveness of differential drag; this is intuitively expected, as a lower ACPL leads to more CAMs against chasers with large covariances, which require larger manoeuvres. A particularly marked drop can be seen at and above $h = 500$ km, with an increase in Δt_{CAM} of around 1 day needed to reach a high level of effectiveness.

3.5 Limitations and Comparison with Literature

In general, comparing the results of this study with [11], one can note that the derived values of η_M are much higher in this study than in [11]. As an example, for $\beta_{max}/\beta_{min} = 3$, $\Delta t_{CAM} = 3$ days, and $600\text{ km} \leq h < 700$ km, they report $\eta_M = 11\%$. In contrast, as seen in Fig. 6, for the same conditions, the small satellite case in this study ($\beta_{max}/\beta_{min} \approx 2.7$) reports $\eta_M > 95\%$. Unfortunately, no reports on η_Q are available in [11], precluding a comparison.

The reason for this large discrepancy is still being investigated. However, it is important to note the differences between the studies; whilst ARES still bases its results off of binned CDM statistics, the methodology varies significantly from [11], with more data being user-defined and simulated rather than relying purely on averaged statistics [12]. However, a drawback of this is that not every effect is modelled. Notably, while ARES can model the decrease in manoeuvre size when an earlier decision time is chosen, and the increase in covariances at Time of Closest Approach (TCA), it does not take into account the increase in covariance at TCA due to the CAM itself.

Another limitation of ARES is that it does not take into account how long before the Time of Closest Approach (TCA) an event becomes critical. Thus, it cannot quantify the number of CAMs that will be missed due to late detections. This should be explored further in future work, as this would have a particularly large effect due to the long manoeuvre times associated with differential drag. However, this was also not explored in [11], so cannot be the source of the differences.

Another example of this difference in methodology is present in the approach taken for β. According to Eq. 1, F11the second derivative of the achievable separation distance is driven by the absolute change in β, leading to the definition of $\Delta\beta_{CAM}$ shown in Eq. 5. On the other hand, [11] uses a dimensionless proxy for the change in β, defined as the ratio $\Delta\beta_{CAM} = \beta_{max}/\beta_{min} - 1$. Furthermore, based on Eq. 1, given the effectiveness scaling based on the absolute difference in β, one would expect that for a fixed ratio of β_{max}/β_{min}, η_M would be directly correlated with β_{min} or β_{max}; however, their results suggest little effect. Assuming the relation in Eq. 1 is correct, this could potentially be explained by the operational uncertainty and variation in β making trends hard to distinguish, but this would need further study to confirm.

It is also interesting to note that in contrast to the results shown in Fig. 3, the results of [11] only show a weak correlation with F10.7 solar index. Whilst the effect of solar flux on the atmospheric density are indisputable, it is possible that the increase in covariance and variance in β during these high solar activity periods reduces any change in effectiveness. As previously mentioned, ARES does not currently have the ability to model these changes, which might be the cause of these discrepancies.

Finally, a very important difference between the studies is the assumed test case geometry change. As noted in Section 2.2, in contrast to the approach of this paper [11] assumes that the spacecraft nominally remains at β_{min}, and that $\beta_{CAM} = \beta_{max}$. Whilst allowing for the maximum change in inverse ballistic coefficient, this manoeuvre methodology only allows for manoeuvring in one direction, which based on the manoeuvre geometry can increase the ΔV required. This could contribute to the much lower η_M, although further analysis would be needed to confirm this.

All in all, the disagreement between the results clearly sets out the need for further analysis, in order to understand the reasons for these discrepancies, and to arrive at more concrete conclusions on the effectiveness of differential drag. However, overall, it is important to note that even if the CAM timeliness requirements described by [2] might not always be reachable solely using differential drag, the results of this paper suggest that differential drag could be used as an additional measure to reduce the collision risk, especially when other manoeuvring methods might not be available. This would of course need to be analysed on a case-to-case basis, and operational factors such as the ones described in Section 1.1 would need to be considered. These could make other, alternatives such as reducing the collision cross-sectional area, more viable.

4 CONCLUSIONS

To conclude, a set of scripts and a simulation pipeline was created using the ARES tool, leveraging the implementation of differential drag equations, in order to derive statistics of the effectiveness of differential drag at different altitudes, and for different test cases.

The results were presented, and as expected, large variations were seen with the altitude and lead the time. A 3U CubeSat with large solar panels showed impressively high effectiveness until around 550km, whilst the larger spacecraft started to drop in effectiveness already at lower altitudes. However, these results suggest that even if differential drag might not be best as the main way to perform a CAM, it could potentially be a viable way to nonetheless reduce the risk of collision.

Several of the assumptions were discussed, as they made the analysis tractable, but of course limited the fidelity of the results. Additionally, recurring trends were seen for the test cases at specific altitudes, which are to be analysed in more detail to derive a satisfactory explanation.

Finally, large discrepancies were seen between the results of this paper and another in the literature. This should be explored further, through the simulation of more test cases, environmental conditions, and orbits, in order to be able to have a more conclusive verdict on the effectiveness of differential drag.

5 ACKNOWLEDGEMENTS

Part of this work was completed during a past secondment of the first author to the UK Space Agency, within the Office of the Chief Engineer (OCE), whilst he was employed by the European Space Agency.

6 REFERENCES

[1] IADC WG3 members, ‘Protection manual’, 2014.

[2] ESA Space Debris Mitigation Working Group, ‘ESA Space Debris Mitigation Requirements’, Oct. 30, 2023. Accessed: Mar. 19, 2025. [Online]. Available: https://sdup.esoc.esa.int/documents/download/ESSB-ST-U-007_Issue_1_30October2023.pdf

[3] Zero Debris Stakeholders, ‘Zero Debris Technical Booklet’, Dec. 2024. Accessed: Mar. 19, 2025. [Online]. Available: https://esamultimedia.esa.int/docs/spacesafety/Zero_Debris_Technical_Booklet.pdf

[4] C. D. Bussy-Virat, A. J. Ridley, A. Masher, K. Nave, and M. Intelisano, ‘Assessment of the Differential Drag Maneuver Operations on the CYGNSS Constellation’, *IEEE J Sel Top Appl Earth Obs Remote Sens*, vol. 12, no. 1, 2019, doi: 10.1109/JSTARS.2018.2878158.

[5] C. Foster *et al.*, ‘Constellation phasing with differential drag on planet labs satellites’, in *Journal of Spacecraft and Rockets*, 2018. doi: 10.2514/1.A33927.

[6] F. Turco, C. Traub, S. Gaißer, J. Burgdorf, S. Klinkner, and S. Fasoulas, ‘An analysis tool for collision avoidance manoeuvres using aerodynamic drag’, *Acta Astronaut*, vol. 211, 2023, doi: 10.1016/j.actaastro.2023.05.038.

[7] 18th & 19th Space Defense Squadron, ‘Spaceflight Safety Handbook for Satellite Operators’, Apr. 2023. Accessed: Mar. 19, 2025. [Online]. Available: https://www.space-track.org/documents/SFS_Handbook_For_Operators_V1.7.pdf

[8] N. Griffith, R. Bhatia, R. T. Nallapu, M. Siegers, V. Mallik, and C. Rosner, ‘Small Satellite Collision Risk Mitigation Using Differential Drag’, in *Proceedings of the International Astronautical Congress, IAC*, 2021.

[9] S. Hull, A. Shelton, and D. Richardson, ‘DIFFERENTIAL DRAG DEMONSTRATION: A POST-MISSION EXPERIMENT WITH THE EO-1 SPACECRAFT’, Orlando, FL, USA, Nov. 2017. Accessed: Mar. 19, 2025. [Online]. Available: https://ntrs.nasa.gov/citations/20170011151

[10] S. R. Omar and R. Bevilacqua, ‘Spacecraft collision avoidance using aerodynamic drag’, *Journal of Guidance, Control, and Dynamics*, vol. 43, no. 3, 2020, doi: 10.2514/1.G004518.

[11] James R. Clark and Dolan E. Highsmith, ‘Decision Aid for Conjunction Risk Mitigation by Differential Drag’, in *Astrodynamics Specialist Conference*, Broomfield, CO: Preprint, Aug. 2024.

[12] N. Sánchez-Ortiz, M. Belló-Mora, and H. Klinkrad, 'Collision avoidance manoeuvres during spacecraft mission lifetime: Risk reduction and required ΔV', *Advances in Space Research*, vol. 38, no. 9, 2006, doi: 10.1016/j.asr.2005.07.054.

[13] Philippe Meyers *et al.*, 'The Debris Mitigation Facility: Developments, Conclusions, Use Cases and Way Forward', in *9th European Conference on Space Debris,* Bonn, Apr. 2025.

[14] M. Hülsmann *et al.*, 'Debris collision avoidance by means of attitude control-in-flight demonstration with TET-1', *Journal of Space Safety Engineering*, vol. 6, no. 4, 2019, doi: 10.1016/j.jsse.2019.09.003.

[15] D. Evans and A. Donati, 'The esa ops-sat mission: Don't just say there is a better way, fly it and prove it', in *15th International Conference on Space Operations, 2018*, 2018. doi: 10.2514/6.2018-2730.

[16] J. T. Emmert *et al.*, 'NRLMSIS 2.1: An Empirical Model of Nitric Oxide Incorporated Into MSIS', *J Geophys Res Space Phys*, vol. 127, no. 10, 2022, doi: 10.1029/2022JA030896.

[17] 'Proceedings of the Magnetic Coupling of the Solar Atmosphere Euroconference and IAU Colloquium 188: SOLMAG 2002', 2002.

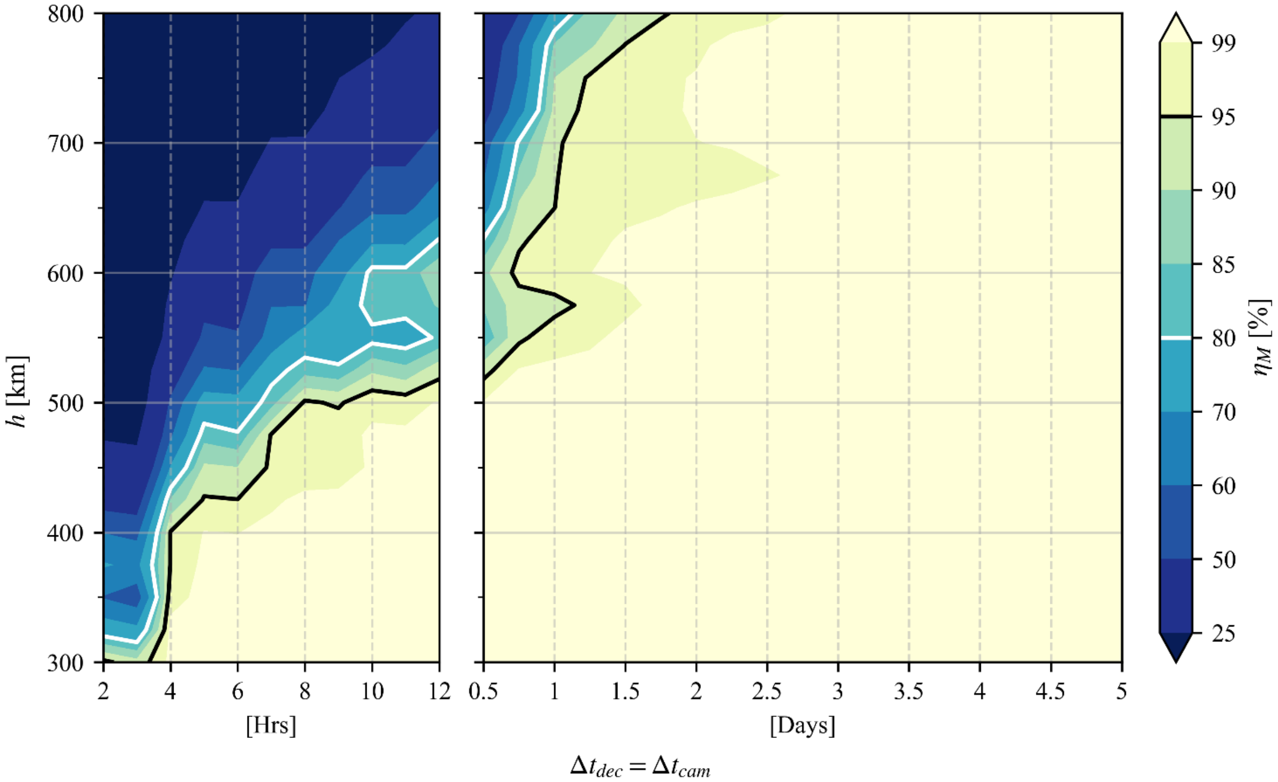

Figure 4. Percentage of CAMs that are possible when solely using differential drag, for the CubeSat test case, $i = SSO$, ACPL=1E-4.

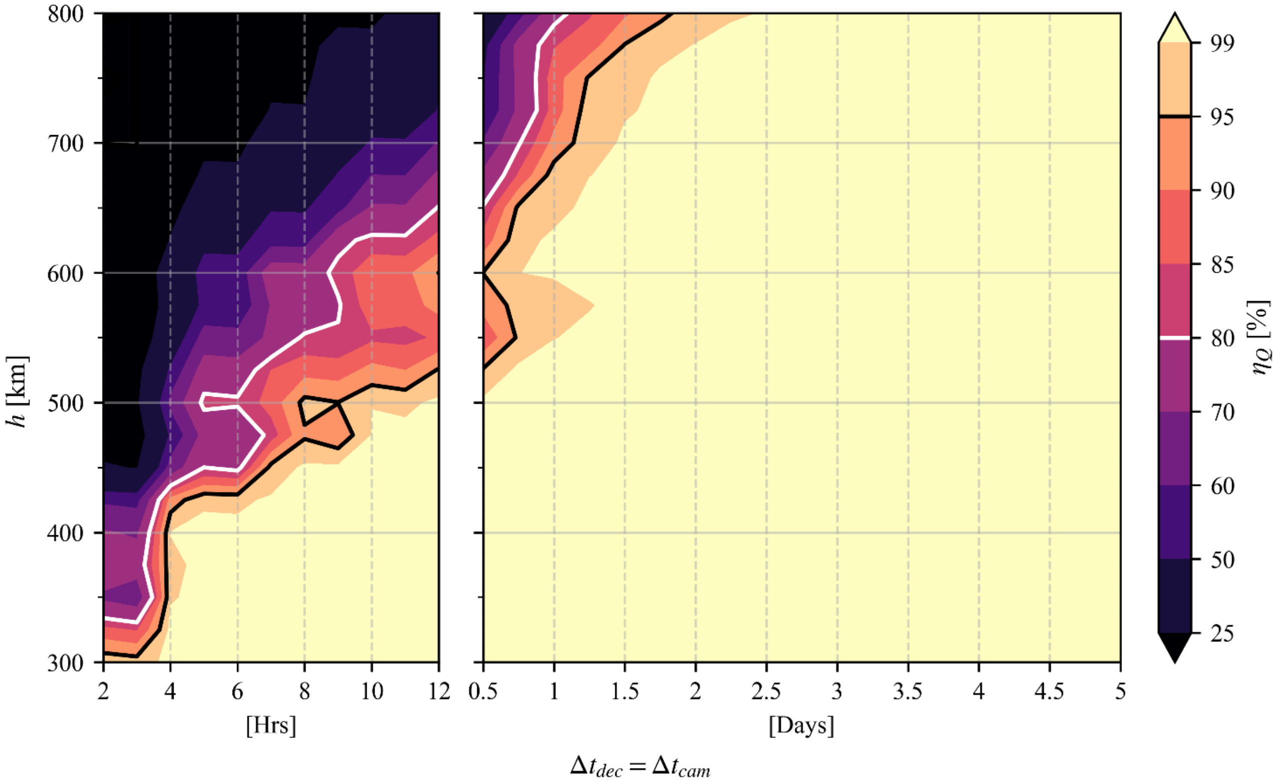

Figure 5. Percentage of risk reduction that is possible relative to impulsive manoeuvres when solely using differential drag, for the CubeSat test case, $i = SSO$, ACPL=1E-4.

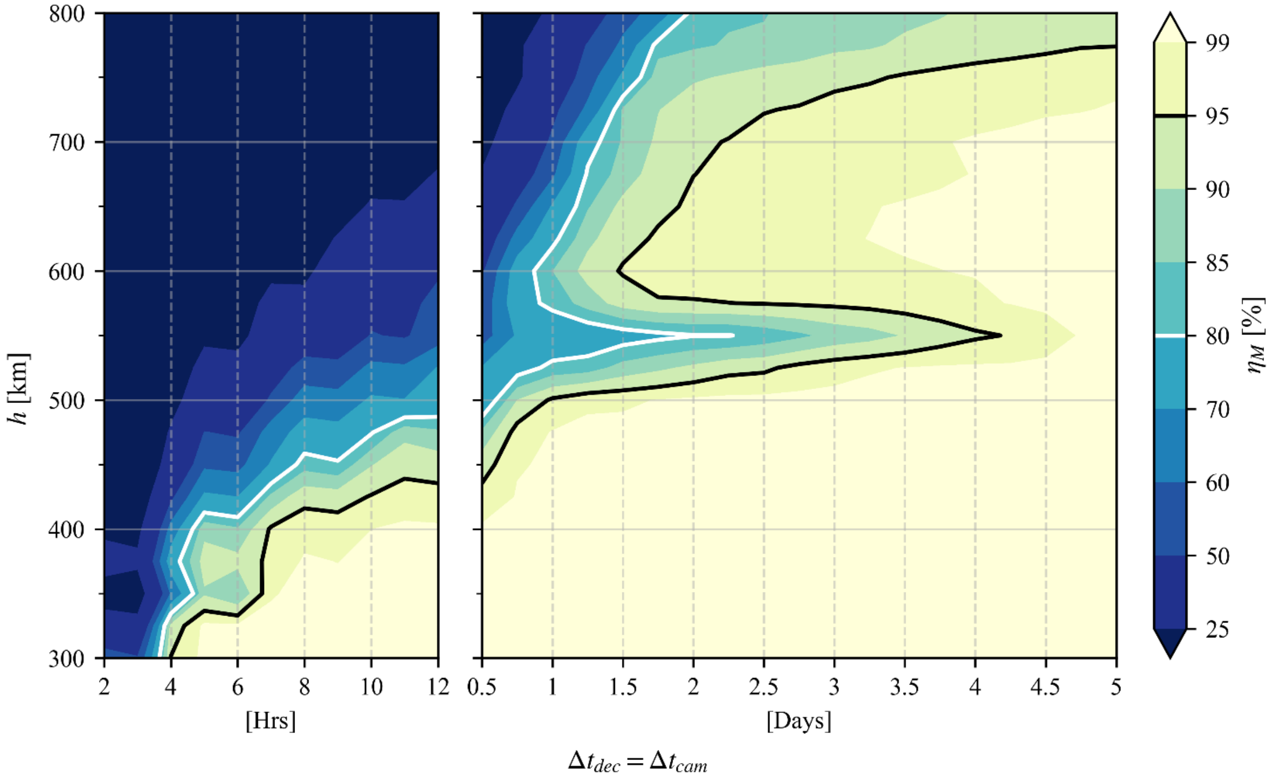

Figure 6. Percentage of CAMs that are possible when solely using differential drag, for the small satellite test case, $i = SSO$, ACPL=1E-4.

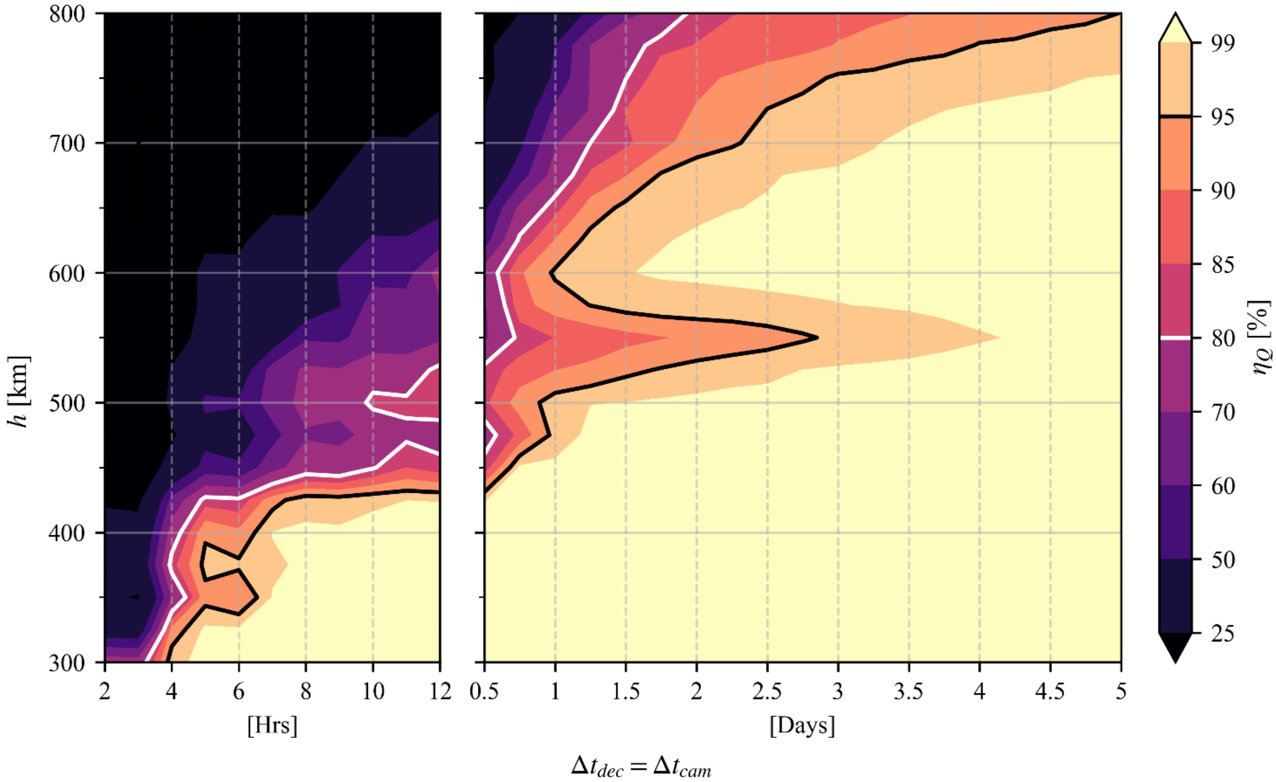

Figure 7. Percentage of risk reduction that is possible relative to impulsive manoeuvres when solely using differential drag, for the small satellite test case, $i = SSO$, ACPL=1E-4.

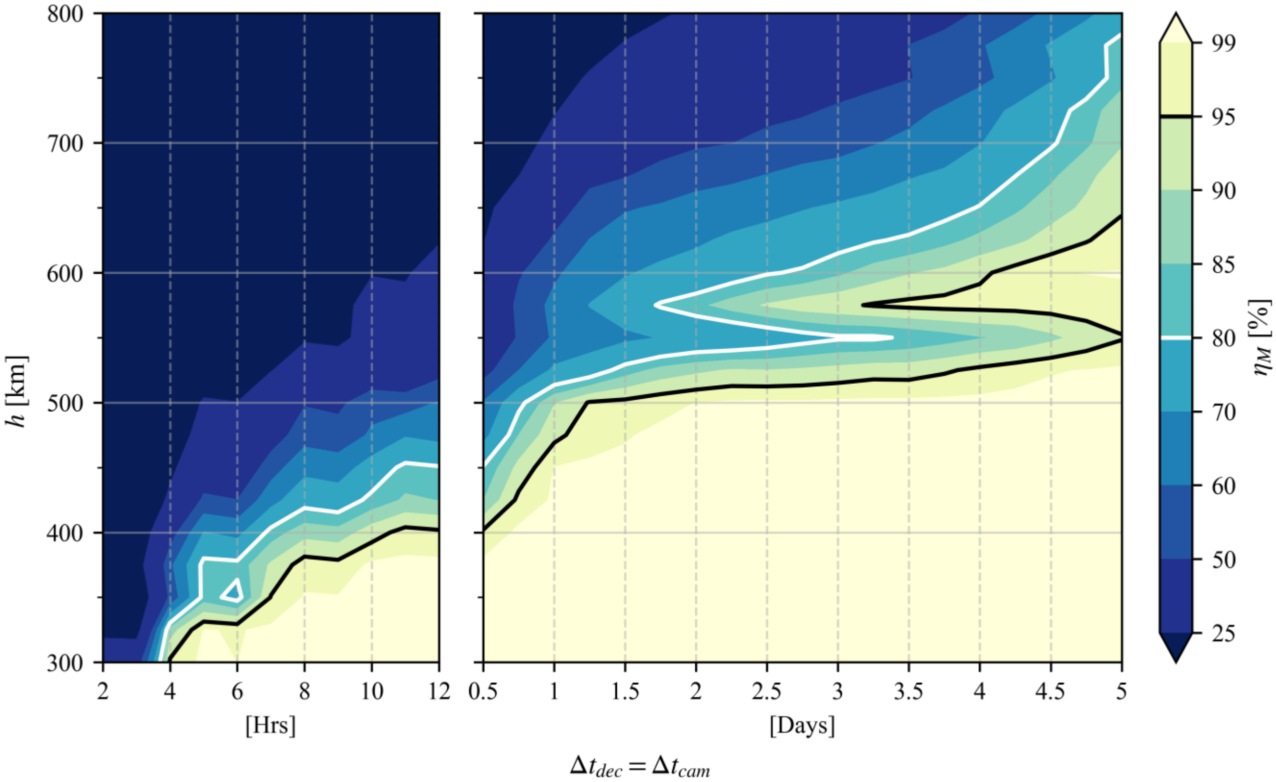

Figure 8. Percentage of CAMs that are possible when solely using differential drag, for the large satellite test case, $i = SSO$, ACPL=1E-4.

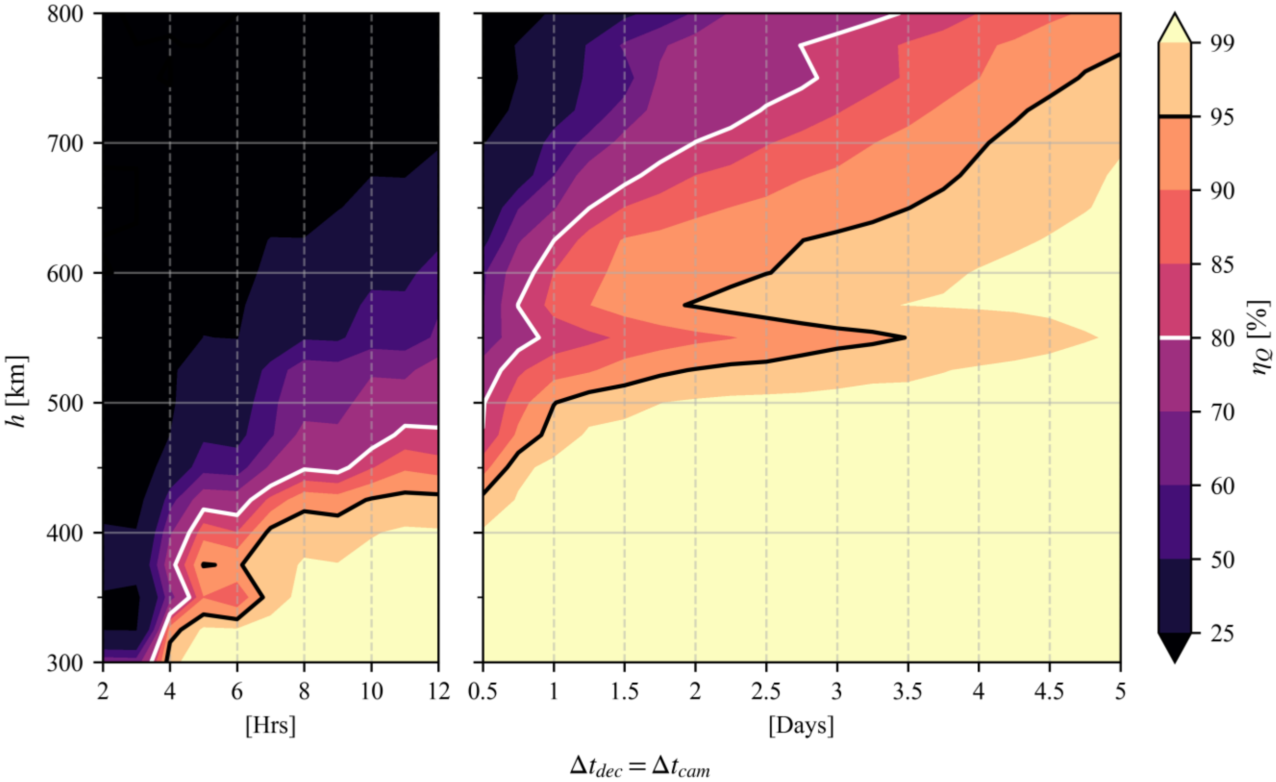

Figure 9. Percentage of risk reduction that is possible relative to impulsive manoeuvres when solely using differential drag, for the large satellite test case, $i = SSO$, ACPL=1E-4.

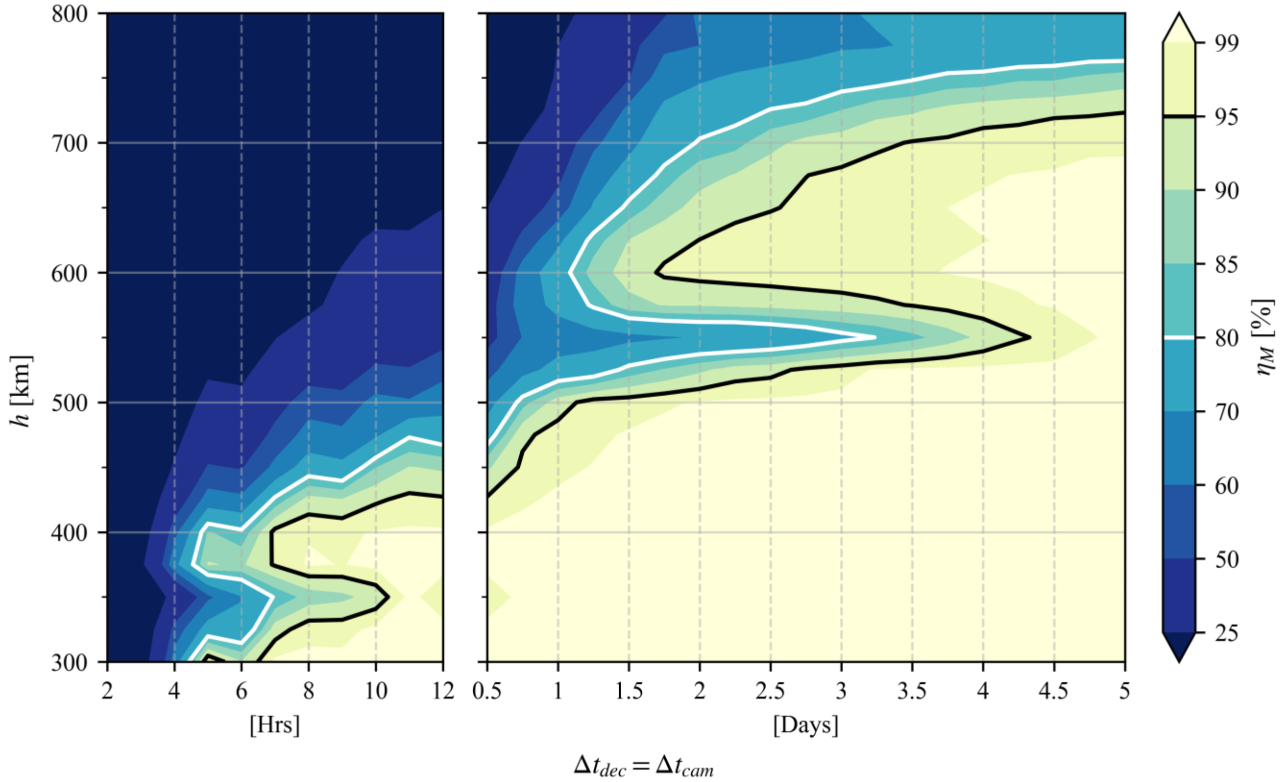

Figure 10. Percentage of CAMs that are possible when solely using differential drag, for the small satellite test case, $i = 53°$, ACPL=1E-4.

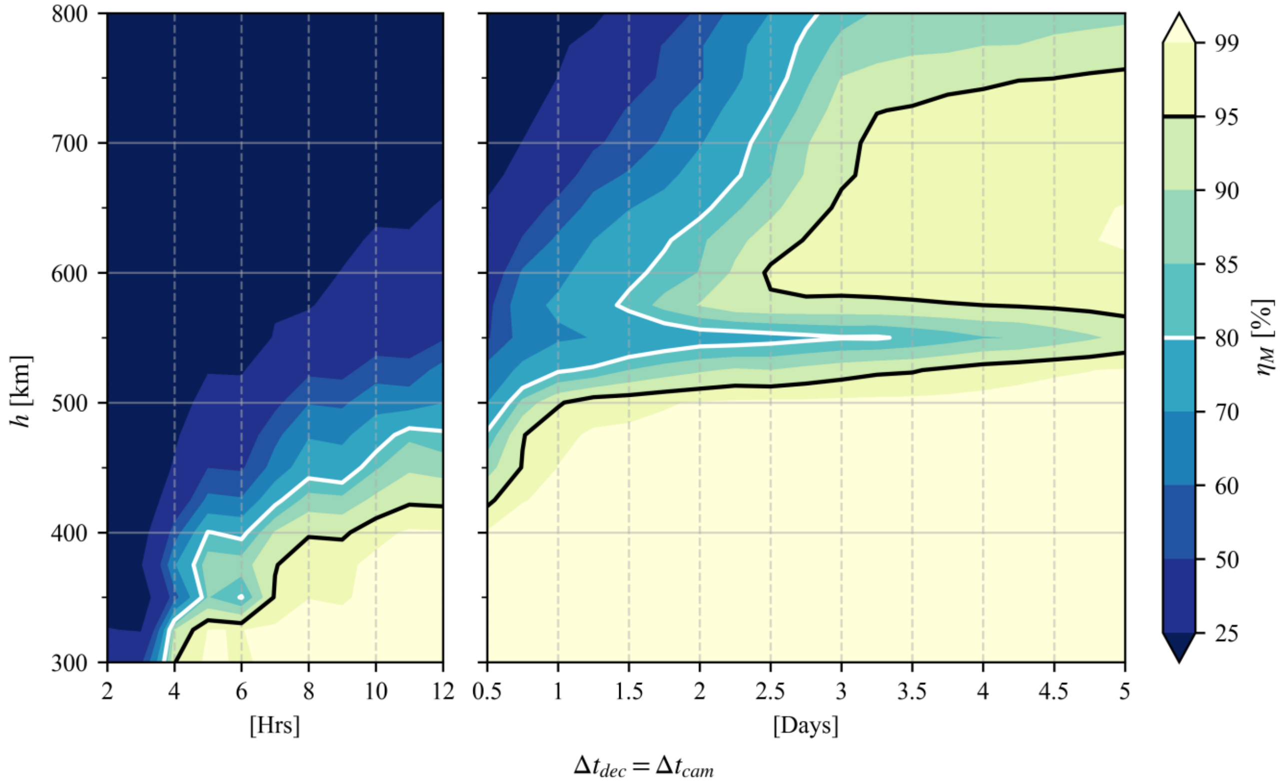

Figure 11. Percentage of CAMs that are possible when solely using differential drag, for the small satellite test case, $i = SSO$, ACPL=4E-5.